

# Surface polaritons in magnetic metamaterials from perspective of effective-medium and circuit models

Cite as: J. Appl. Phys. **117**, 163910 (2015); <https://doi.org/10.1063/1.4919072>

Submitted: 13 October 2014 . Accepted: 14 April 2015 . Published Online: 27 April 2015

K. Hadjicosti , O. Sydoruk, S. A. Maier, and E. Shamonina



View Online



Export Citation



CrossMark

## ARTICLES YOU MAY BE INTERESTED IN

[Circuit model optimization of a nano split ring resonator dimer antenna operating in infrared spectral range](#)

Journal of Applied Physics **116**, 164311 (2014); <https://doi.org/10.1063/1.4900479>

[Magnetoinductive waves in one, two, and three dimensions](#)

Journal of Applied Physics **92**, 6252 (2002); <https://doi.org/10.1063/1.1510945>

[Experiments on adjustable magnetic metamaterials applied in megahertz wireless power transmission](#)

AIP Advances **5**, 017142 (2015); <https://doi.org/10.1063/1.4907043>

Applied Physics Reviews  
Now accepting original research

2017 Journal  
Impact Factor:  
**12.894**



# Surface polaritons in magnetic metamaterials from perspective of effective-medium and circuit models

K. Hadjicosti,<sup>1</sup> O. Sydoruk,<sup>1,a)</sup> S. A. Maier,<sup>2</sup> and E. Shamonina<sup>3</sup>

<sup>1</sup>*Optical and Semiconductor Devices Group, Department of Electrical and Electronic Engineering, Imperial College London, South Kensington Campus, London SW7 2AZ, United Kingdom*

<sup>2</sup>*Nanoplasmonics Group, Department of Physics, Imperial College London, South Kensington Campus, London SW7 2AZ, United Kingdom*

<sup>3</sup>*Department of Engineering Science, University of Oxford, Parks Road, Oxford OX1 3PJ, United Kingdom*

(Received 13 October 2014; accepted 14 April 2015; published online 27 April 2015)

Surface waves are responsible for many phenomena occurring in metamaterials and have been studied extensively. At the same time, the effects of inter-element coupling on surface electromagnetic waves (polaritons) remain poorly understood. Using two models, one relying on the effective-medium approximation and the other on equivalent circuits, we studied theoretically surface polaritons propagating along an interface between air and a magnetic metamaterial. The metamaterial comprised split rings that could be uncoupled or coupled to each other in the longitudinal or transverse directions (along or perpendicular to the propagation direction). A metamaterial without inter-element coupling supported a single polariton. When a moderate longitudinal coupling was included, it changed the wave dispersion only quantitatively, and the results of the effective-medium and the circuit models were shown to agree at low wavenumbers. However, the presence of a transverse coupling changed the polariton dispersion dramatically. The effective-medium model yielded two branches of polariton dispersion at low values of the transverse coupling. As the coupling increased, both polaritons disappeared. The validity of the effective-medium model was further tested by employing the circuit model. In this model, surface polaritons could exist in the presence of a transverse coupling only if the boundary layer of the metamaterial included additional impedances, which could become non-Foster. The results reveal that the inter-element coupling is a major mechanism affecting the properties of the polaritons. They also highlight the limitations of using bulk effective-medium parameters for interface problems in metamaterials. © 2015 AIP Publishing LLC. [<http://dx.doi.org/10.1063/1.4919072>]

## I. INTRODUCTION

Ever since the pioneering papers by Pendry *et al.* on the permittivity of a wire medium<sup>1</sup> and the permeability of the split-ring resonator,<sup>2</sup> the development of effective-medium theories has been on the forefront of the metamaterial research. The task is to describe the interaction of an electromagnetic wave with a material using macroscopic parameters, such as permittivity and permeability. The problem is complicated even for natural materials, let alone for artificial ones, whose constituent elements are larger, their number is smaller, and that have varying electric and magnetic properties.<sup>3</sup> Considerable progress has nevertheless been achieved, and the existing effective-medium models for metamaterials have many universally recognized properties. For example, the sought-after effect of negative refraction by means of negative permittivity and permeability should be accompanied by frequency dispersion.<sup>4</sup> Such dispersion is most commonly described by a resonant Drude-Lorentz (e.g., permeability of split rings) or a non-resonant Drude (e.g., permittivity of a wire medium) expressions.

Spatial dispersion—a dependence of the effective parameters on the wavevector—attracted less attention in the past. The classical treatise is by Agranovich and Ginzburg<sup>5</sup> who studied the effect in a generic way and for natural

materials well before the subject of metamaterials emerged. Spatial dispersion in metamaterials has been studied by Silveirinha, Belov, Simovski, and co-authors,<sup>6–13</sup> mostly for wire media but also for other metamaterials. In solid-state plasmas, closely related to the field of plasmonics, spatial dispersion may appear as a result of the electron thermal movement<sup>14</sup> or a dc current.<sup>15</sup>

On the other hand, spatial dispersion appears also as a result of an interaction between metamaterial elements by their electric and magnetic near fields.<sup>16</sup> In the metamaterial context, the subject has been developed extensively by Solymar, Shamonina, and co-authors (see e.g., Refs. 17–20) for magnetic coupling between split-ring resonators, although earlier studies were also conducted for other applications.<sup>21–23</sup> Shamonina<sup>24</sup> has recently derived an expression for the magnetic permeability of a metamaterial comprising coupled split-ring resonators. The model relied on an earlier work by Syms *et al.*,<sup>25</sup> who described an electromagnetic wave interacting with a metamaterial as a periodically loaded transmission line. Shamonina also derived the dispersion relation for surface electromagnetic waves propagating along an air-metamaterial interface, and called them magnetoinductive polaritons. Surface polaritons on magnetic metamaterials were also studied by Gollub *et al.*,<sup>26</sup> those on spatially dispersive wire media by Shapiro *et al.*,<sup>27</sup> and those on magnetic plasmas by Ilin *et al.*<sup>28</sup>

<sup>a)</sup>Electronic mail: osydoruk@imperial.ac.uk

The work of Shamonina<sup>24</sup> concentrated on surface polaritons on metamaterials with longitudinal coupling only (along the propagation direction). It discussed the polariton properties using the effective-medium approximation and electromagnetic boundary conditions, although the bulk permeability was derived from an equivalent circuit. The present paper concentrates on the role of the transverse inter-element coupling (perpendicular to the surface). It considers the surface polaritons from the point of view of both the effective-medium and the equivalent-circuit models. Section II presents the configurations and the circuit model leading to a spatially dispersive tensor of the bulk magnetic permeability. Section III presents the effective-medium approximation leading to a surface-polariton dispersion relation. It discusses the dispersion for different lattice geometries and reveals limitations of the effective-medium approach. Section IV analyses these limitations further using a full equivalent circuit. Based on the results of both models, Sec. V draws conclusions.

## II. SPATIAL DISPERSION OF THE EFFECTIVE PERMEABILITY IN A BULK METAMATERIAL

Following Syms *et al.*<sup>25</sup> and Shamonina,<sup>24</sup> this section discusses how an electromagnetic wave interacts with a bulk split-ring metamaterial. It also derives an expression for the permeability tensor. In a conventional manner, we present split rings as *LC*-resonators with the inductance  $L$  and the capacitance  $C$  so that the angular resonant frequency is  $\omega_0 = 1/\sqrt{LC}$ . Two closely placed rings can become magnetically coupled to each other, and we describe the coupling by a coefficient  $\kappa = 2M/L$ , where  $M$  is the mutual inductance. The sign and the magnitude of the coupling coefficient depend on the positions of the rings relative to each other. For example, the coupling coefficient is positive in the axial configuration [Fig. 1(a), the rings' centers and normals lying on the same axis] and negative in the planar configuration [Fig. 1(b), the rings lying in the same plane]. It can be zero when the rings lie in two perpendicular planes in a T-configuration [Fig. 1(c)], and when they lie in two parallel planes with their centers shifted by a particular distance [Fig. 1(d)].<sup>29</sup> Also, the coupling becomes weaker as the distance between the rings increases. In a metamaterial comprising many elements, this property often allows one to neglect all but the nearest-neighbor couplings.

Here, we consider two-dimensional metamaterials with elements oriented along the  $x$ - and  $z$ -axes, see Fig. 2(a). The inter-element coupling is then characterized by four coupling coefficients:  $\kappa_{ax}$  and  $\kappa_{az}$  between elements in the axial

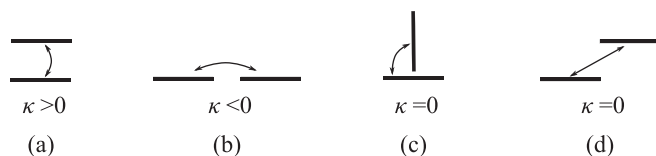


FIG. 1. The magnetic coupling coefficient between two rings depends on their orientation. It is positive in the axial configuration (a), negative in the planar configuration (b), and zero in the T- (c) and the shifted configuration (d).

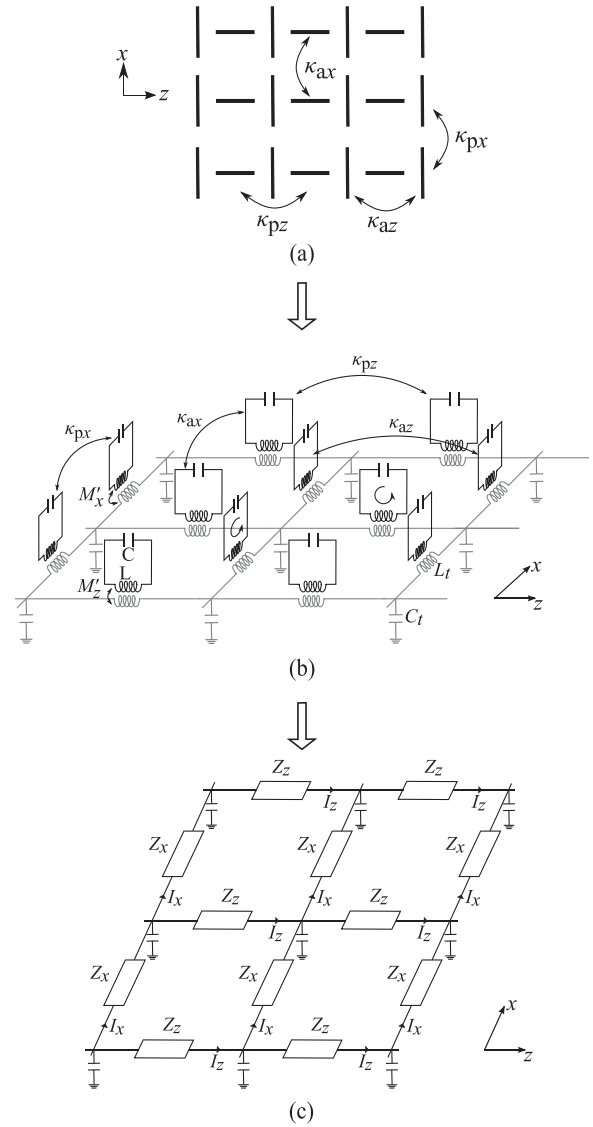


FIG. 2. A magnetic metamaterial comprising split rings (a) can be described by an array of coupled *LC*-resonators, whereas the electromagnetic wave can be seen as propagating along an *LC*-transmission line (b). The split rings load the transmission line allowing us to describe the metamaterial by an equivalent circuit (c).

configuration in the transverse  $x$ - and longitudinal  $z$ -direction, respectively, and the analogous  $\kappa_{px}$  and  $\kappa_{pz}$  between elements in the planar configuration.

We describe the propagation of the electromagnetic wave by a two-dimensional *LC*-transmission line with the inductance  $L_t = \mu_0 d$  and the capacitance  $C_t = \varepsilon_0 d$ , see Fig. 2(b). Here,  $\mu_0$  and  $\varepsilon_0$  are the vacuum permeability and permittivity, and  $d$  is the unit cell size.

A TE wave propagating along the  $z$ -axis has the magnetic-field components  $H_x$  and  $H_z$  and the electric-field component  $E_y$ . The  $H_x$  component interacts with the metamaterial elements whose normals are along the  $x$ -axis, whereas the  $H_z$  component interacts with the elements oriented perpendicular to the  $z$ -axis. Both interactions can be described by mutual inductances  $M'_x$  and  $M'_z$ , see Fig. 2(b). The corresponding coupling coefficients (also known as the fill factors) are  $q_{x(z)}^2 = M_{x(z)}'^2 / LL_t$ .

Referring the impedances of the split rings to the transmission line, we obtain<sup>24</sup> the equivalent circuit shown in Fig. 2(c) with

$$\begin{aligned}\frac{Z_x}{j\omega L_t} &= 1 - \frac{q_x^2}{1 - \frac{\omega_0^2}{\omega^2} + \kappa_{az} \cos(k_z d) + \kappa_{px} \cos(k_x d)}, \\ \frac{Z_z}{j\omega L_t} &= 1 - \frac{q_z^2}{1 - \frac{\omega_0^2}{\omega^2} + \kappa_{ax} \cos(k_x d) + \kappa_{pz} \cos(k_z d)},\end{aligned}\quad (1)$$

where  $\omega$  is the angular frequency, and  $k_z$  and  $k_x$  are the longitudinal and the transverse wavenumbers, respectively.

Using the nodal analysis, we obtain for this circuit

$$\begin{aligned}V_{l+1,m} - V_{l,m} &= -Z_x I_{x,l,m}, \\ V_{l,m+1} - V_{l,m} &= -Z_z I_{z,l,m},\end{aligned}\quad (2)$$

where the subscripts  $l$  and  $m$  denote the nodes in the  $x$ - and  $z$ -directions, respectively. The voltages  $V$  are across the capacitors, and the currents  $I_x$  and  $I_z$  flow through the impedances  $Z_x$  and  $Z_z$  [see Fig. 2(c)]. Making a transition from the circuit to a homogeneous material, we can relate the currents and voltages to the field quantities as  $V = E_y d$ ,  $I_x = H_z d$  and  $I_z = -H_x d$ . On the other hand, Maxwell's equations for the TE wave can be written in the form

$$\begin{aligned}\frac{\partial H_x}{\partial z} - \frac{\partial H_z}{\partial x} &= j\omega \epsilon_0 E_y, \\ \frac{\partial E_y}{\partial z} &= j\omega \mu_0 \mu_x H_x, \\ \frac{\partial E_y}{\partial x} &= -j\omega \mu_0 \mu_z H_z.\end{aligned}\quad (3)$$

Here, we introduced the effective permeabilities  $\mu_x$  and  $\mu_z$  as

$$\mu_x = \frac{Z_z}{j\omega L_t}, \quad \mu_z = \frac{Z_x}{j\omega L_t}. \quad (4)$$

These expressions can be reduced to several known special cases. First, if the metamaterial elements are uncoupled, the  $x$ - and  $z$ -components of the permeability are, as they should, in the standard Drude-Lorentz form. A correction due to the coupling can be made assuming  $k_{x(z)} d \ll 1$  so that  $\cos(k_{x(z)} d) \approx 1$ . Then  $\mu_x$ , for example, can be written as

$$\mu_x \approx 1 - \frac{q_z^2}{1 - \frac{\omega_0^2}{\omega^2} + \kappa_{ax} + \kappa_{pz}}, \quad (5)$$

which is the nearest-neighbor form of the expression derived by Gorkunov *et al.*<sup>30</sup>

The longitudinal and transverse wavenumbers  $k_z$  and  $k_x$  in a bulk metamaterial are linked together via the dispersion relation, which has the form

$$\frac{4}{Z_z} \sin^2 \frac{k_z d}{2} + \frac{4}{Z_x} \sin^2 \frac{k_x d}{2} = -j\omega C_t. \quad (6)$$

The dispersion relation for the transmission line representing air has the same form but with  $Z_z = Z_x = j\omega L_t$  (implying  $\mu_x = \mu_z = 1$ ).

We are interested here in polaritons that have nonzero components of the magnetic field. Solutions with zero  $H_x$  or  $H_z$  (and, hence,  $I_z$  or  $I_x$ ) are also possible; and their dispersion relations are  $\mu_x = 0$  or  $\mu_z = 0$ . These solutions, as follows from Eq. (1), correspond to the magnetoinductive waves propagating on two-dimensional metamaterial arrays.<sup>31</sup> Such waves can also propagate along an interface between two metamaterials and were discussed in Ref. 20.

### III. EFFECTIVE-MEDIUM MODEL OF SURFACE POLARITONS

Relying on an effective-medium model, this section describes the surface polaritons propagating along the interface between a metamaterial and air. It concentrates in particular, on the effects of the inter-element coupling. Assuming that the metamaterial is a homogeneous medium characterised by the permeabilities  $\mu_x$  and  $\mu_z$ , we can rewrite the bulk dispersion relation Eq. (6) in the form

$$\mu_z k_z^2 + \mu_x k_{x2}^2 = \mu_z \mu_x k_0^2, \quad (7)$$

where  $k_0 = \omega/c$  with the vacuum light velocity  $c$ , and the subscript 2 denotes the quantities in the metamaterial. Denoting the quantities in air by the subscript 1, we have

$$k_z^2 + k_{x1}^2 = k_0^2. \quad (8)$$

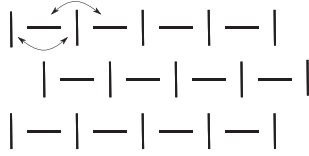
We place the interface between air and the metamaterial at  $x=0$  and consider surface waves propagating along the  $z$ -direction. For the effective medium, we assume that the standard Maxwell boundary conditions apply, yielding  $\mu_z k_{x1} = k_{x2}$ . This equation can be rewritten, using Eqs. (7) and (8), as<sup>24</sup>

$$k_z^2 = k_0^2 \frac{\mu_x (1 - \mu_z)}{1 - \mu_x \mu_z}. \quad (9)$$

Equations (7)–(9) are a system of coupled equations. As Sec. IV shows, it can be alternatively derived directly from the circuit equations assuming small  $k_z d$ . The number of unknowns equals the number of equations, so the system can be solved, albeit generally only numerically. However, if the metamaterial elements are not coupled in the transverse direction ( $\kappa_{ax}, \kappa_{px} = 0$ ), the equations become uncoupled leading to a simple solution  $\omega = \omega(k_z)$ . This situation corresponds to the “brick-wall” metamaterial,<sup>24</sup> see Fig. 3(a). Here, the transverse coupling is eliminated by shifting the neighboring rows by half a period, see also Figs. 1(c) and 1(d). For a numerical example, we took the resonant frequency of the elements as  $\omega_0/(2\pi) = 100$  MHz, the period as  $d = 0.19$  m, and the fill factors as  $q_{x(z)}^2 = 0.2$ . The solid line in Fig. 3(b) shows the dispersion curve of the surface polaritons assuming  $\kappa_{az} = 0.1$  and  $\kappa_{pz} = -0.1$ , whereas the dashed line shows the curve assuming no inter-element coupling at all. The dotted line is the vacuum light line. The presence of this moderate coupling changes the dispersion somewhat, but without a qualitative difference. At low wavenumbers, the dispersion curve shifts downwards so that the surface polaritons can propagate at lower frequencies. At

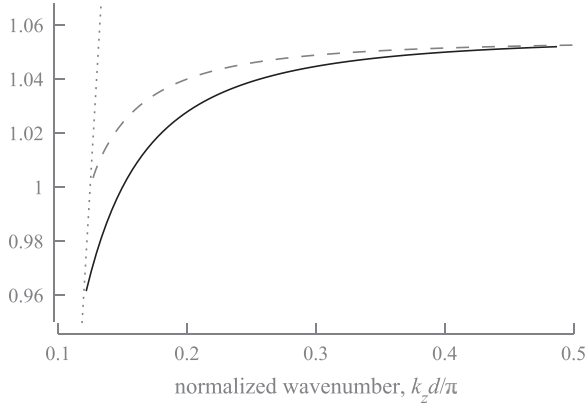


brick wall



$$\begin{aligned}\kappa_{az} &= 0.1 & \kappa_{ax} &= 0 \\ \kappa_{pz} &= -0.1 & \kappa_{px} &= 0\end{aligned}$$

(a)

normalized frequency,  $\omega/\omega_0$ 

(b)

FIG. 3. In the “brick-wall” metamaterial (a), only the longitudinal coupling is present. The surface-polariton dispersion (b) taking the coupling into account (solid line) differs quantitatively from the uncoupled one (dashed line). The dotted line is the light dispersion in vacuum.

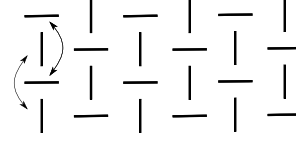
higher wavenumbers, the curves with and without the inter-element coupling hardly differ from each other.

The situation, however, changes dramatically when the inter-element coupling in the direction normal to the interface (i.e., along the  $x$ -axis) exists. For example, a metamaterial with a zero longitudinal but non-zero transverse coupling can be obtained by rotating the “brick-wall” structure by  $90^\circ$  along the  $x$ -axis, see Fig. 4(a). The solid line in Fig. 4(b) shows the dispersion curves corresponding to  $\kappa_{ax} = 0.009$  and  $\kappa_{px} = -0.009$ , whereas the dashed line shows as before the dispersion curve without any inter-element coupling.

Two surface polaritons can now exist. Compared to the original “brick-wall,” the region where they propagate has shrunk both in the frequency and the wavenumber. The coupled dispersion curve lies above the uncoupled one. Compared to the original “brick-wall” (Fig. 3), we reduced the coupling strength in the rotated “brick-wall” (Fig. 4) by more than an order of magnitude. The reason is that the rotated “brick-wall” with a strong transverse coupling supports no polaritons, as will be discussed later.

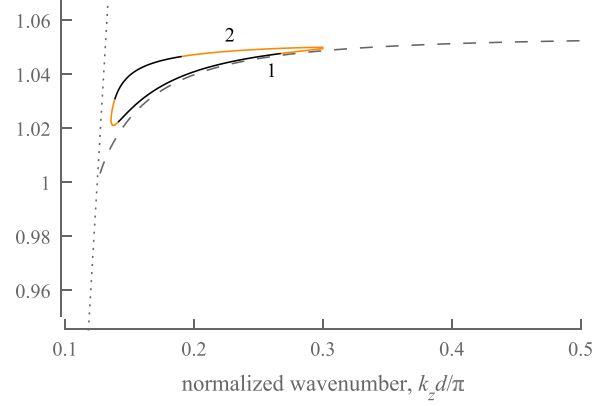
As an example of a metamaterial with both longitudinal and transverse inter-element coupling, we then considered the “fence” structure shown schematically in Fig. 5(a). The solid lines in Fig. 5(b) show the dispersion curves of the surface polaritons for  $\kappa_{az} = 0.1$ ,  $\kappa_{pz} = -0.1$ ,  $\kappa_{ax} = 0.009$ , and  $\kappa_{px} = -0.009$ . They have the same boomerang form as for the rotated “brick-wall,” but with extended ranges of frequencies and wavenumbers. One branch of the coupled

rotated brick wall



$$\begin{aligned}\kappa_{az} &= 0 & \kappa_{ax} &= 0.009 \\ \kappa_{pz} &= 0 & \kappa_{px} &= -0.009\end{aligned}$$

(a)

normalized frequency,  $\omega/\omega_0$ 

(b)

FIG. 4. Rotating the “brick-wall” of Fig. 3 creates a metamaterial with non-zero transverse and zero longitudinal coupling (a). The dispersion diagrams (b) of the surface polaritons with (solid line) and without (dashed line) coupling differ qualitatively from each other. The sections where the frequency derivative of an effective permeability becomes negative (see Fig. 6) are shown in orange.

dispersion lies above the uncoupled one (dashed line), and the other below it.

The dispersion diagrams for both structures with transverse inter-element coupling (rotated “brick-wall” and “fence”) are in the form of a boomerang, cf. Figs. 4(b) and 5(b). At their right and left edges, the polariton group velocity becomes infinitely large. Such a behavior is not uncommon for effective-medium models relying on permittivities and permeabilities, see, for example, Ref. 9. It cannot, however, be expected in passive media and indicates that some approximations of the model fail. In passive lossless media, the frequency derivatives of the effective permeabilities must be positive,<sup>5,10</sup>  $\partial\mu_z/\partial\omega > 0$  and  $\partial\mu_x/\partial\omega > 0$ . For the rotated “brick-wall” metamaterial of Fig. 4, one of the derivatives is negative for the lower branch (mode 1) at small and large values of the wavenumber, as can be seen in Fig. 6(a). For the upper branch (mode 2), the derivative  $\partial\mu_x/\partial\omega$  is negative across a wider range of the wavenumbers. The corresponding regions are shown in orange in Figs. 4(b) and 6. The two modes supported by the “fence” metamaterial behave similarly, see Fig. 5(b). We examine the reason for the breakdown of the effective-medium model in Sec. IV. However, we will first discuss the effects of the transverse coupling on surface polaritons in more detail.

Increasing the transverse inter-element coupling has a detrimental effect on the surface polaritons, as Figs. 7(a) and 7(b) show for the rotated “brick-wall” and the “fence”

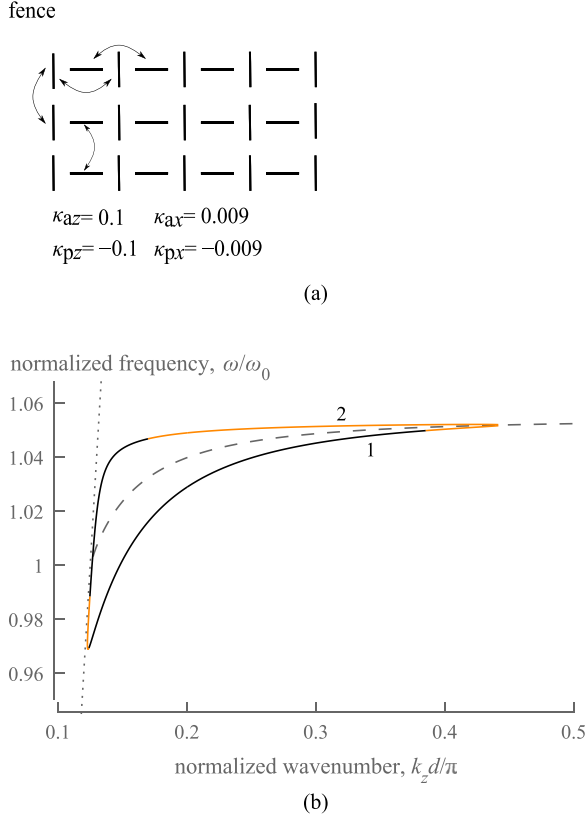


FIG. 5. The “fence” metamaterial (a) has both non-zero longitudinal and non-zero transverse coupling. The dispersion diagram (b) of the surface polaritons (solid lines) has a boomerang shape, similar to that of the rotated “brick-wall” (Fig. 4). It differs from the uncoupled dispersion (dashed line). The sections where the frequency derivative of an effective permeability becomes negative are shown in orange.

metamaterials. They show the same curves as in Figs. 4(b) and 5(b) for  $\kappa_{ax} = |\kappa_{px}| = 0.009$ , but also the curves for a stronger coupling of  $\kappa_{ax} = |\kappa_{px}| = 0.015$  in Fig. 7(a) and for  $\kappa_{ax} = |\kappa_{px}| = 0.05$  and  $0.064$  in Fig. 7(b). For the sections of the dispersion curves shown in black, the frequency derivatives of both effective permeabilities are positive. At least one of them is negative for the sections shown in orange. For both structures, the dispersion diagram dwindles as the transverse coupling increases, and if it exceeds a threshold value, the surface polaritons disappear. This threshold value increases for larger longitudinal coupling.

The penetration depths inside a metamaterial are different for the polaritons corresponding to the two branches of the dispersion diagram. They also depend on the coupling strength. Figures 8(a) and 8(b) show the normalized penetration depth,  $1/(2k_x d)$ , for the rotated “brick-wall” and the “fence” metamaterials at the value of frequency  $\omega/\omega_0 = 1.04$ . For both structures, the waves of mode 1 (denoted by 1 in Figs. 4 and 5) penetrate deeper regardless of the coupling strength. However, as the transverse coupling weakens, the penetration depth of mode 1 increases, while that of mode 2 (denoted by 2 in the dispersion diagrams) decreases.

#### IV. CIRCUIT MODEL OF SURFACE POLARITONS

Section II presented the bulk permeability tensor using an equivalent circuit, but Sec. III discussed surface polaritons

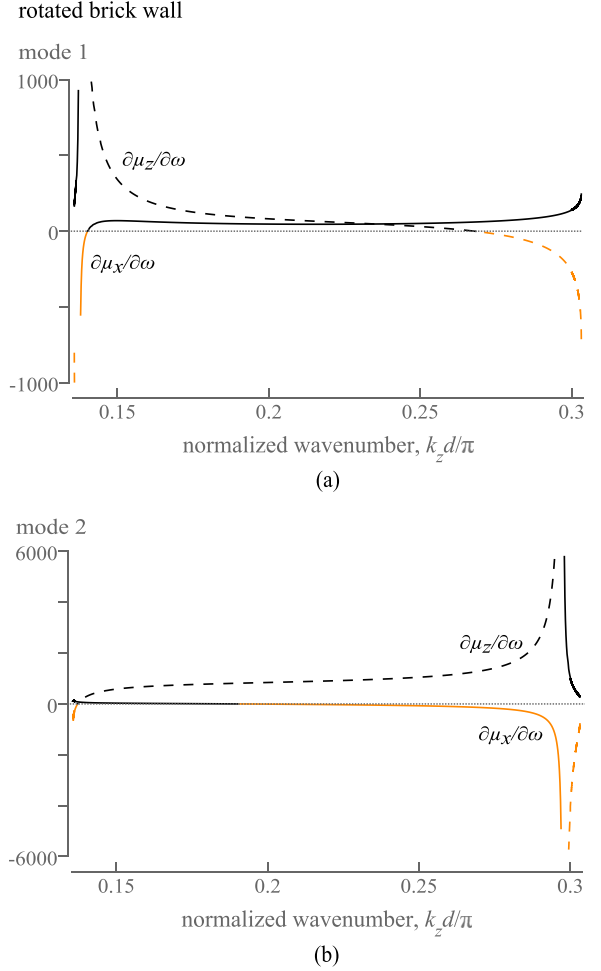


FIG. 6. For the rotated “brick-wall,” the frequency derivatives of the relative permeabilities corresponding to both modes can become negative (shown in orange). This behavior, which cannot be seen in passive lossless metamaterials, suggests that the effective-medium model breaks down.

entirely from the perspective of the effective-medium approximation. However, when the metamaterial elements were coupled to each other in the transverse direction, this approximation appeared to break down for some regions of the polariton dispersion diagram. The frequency derivative of the effective permeability was not positive for every wavenumber, see Fig. 6. To clarify the reasons for this behavior, this section considers the surface polaritons using the full circuit, without the effective-medium approximation. To define an interface between two circuits representing the metamaterial and air, proper unit cells have to be chosen. The best choice is the symmetric unit cells<sup>32,33</sup> shown in Figs. 9(a) and 9(b), resulting in the boundary shown in Fig. 9(c).

The impedances  $Z_x$  and  $Z_z$  are due to the split rings loading the transmission line, see Fig. 2. When the rings are coupled to each other, a change of the impedances in the boundary layer can change the impedances in the whole circuit. It can be shown that, as a result, the metamaterial can support surface eigenwaves only if the impedances at the boundary and in the bulk are the same.

However, the rings at the boundary are missing some neighbors in the transverse direction, which could affect their currents. To compensate for the missing neighbors, the rings

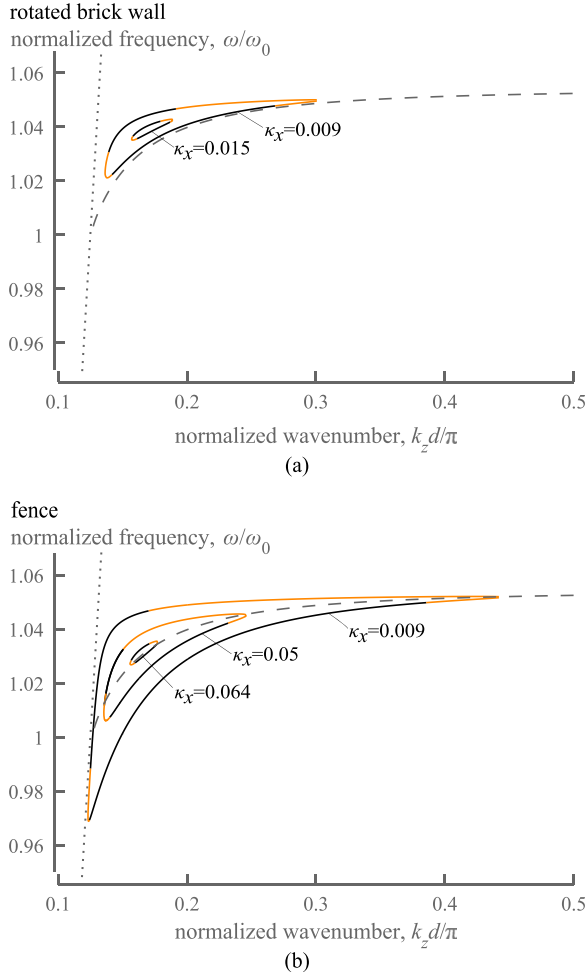


FIG. 7. As the strength of the inter-element coupling increases, the dispersion curves of both the rotated “brick-wall” (a) and the “fence” (b) dwindle. The effect is stronger for the rotated “brick-wall.” The sections where the frequency derivative of an effective permeability becomes negative are shown in orange.

at the boundary must be loaded by additional impedances,  $Z_{Tx}$  and  $Z_{Tz}$ , equal to

$$Z_{Tx} = \frac{Z_x - 2j\omega M_{az} \cos(k_z d) + 2\omega M_{px} \sin(k_{x2} d)}{2}, \quad (10)$$

$$Z_{Tz} = Z_z + j\omega M_{ax} e^{-jk_{x2} d}.$$

The impedance  $Z_{Tx}$  should be added to the rings coupled to the neighbors by  $\kappa_{az}$  and  $\kappa_{px}$ . The impedance  $Z_{Tz}$  should be added to those coupled by  $\kappa_{pz}$  and  $\kappa_{ax}$ . If the transverse coupling is absent (as in the “brick-wall” metamaterial),  $Z_{Tx} = Z_{Tz} = 0$ , and no loading is needed.

The waves in the metamaterial circuit obey Eq. (6), whereas the waves in air circuit obey the same equation but with  $Z_x$  and  $Z_z$  replaced by  $j\omega L_t$ . The presence of the boundary imposes an additional condition that can be obtained, using Kirchhoff’s law, in the form

$$\frac{j\omega L_t}{1 - e^{jk_{x1} d}} + \frac{Z_x}{1 - e^{-jk_{x2} d}} = \frac{Z_x + j\omega L_t}{2}. \quad (11)$$

Here, as before,  $k_{x1}$  and  $k_{x2}$  denote the transverse wavenumbers in the air and metamaterial circuits, respectively.

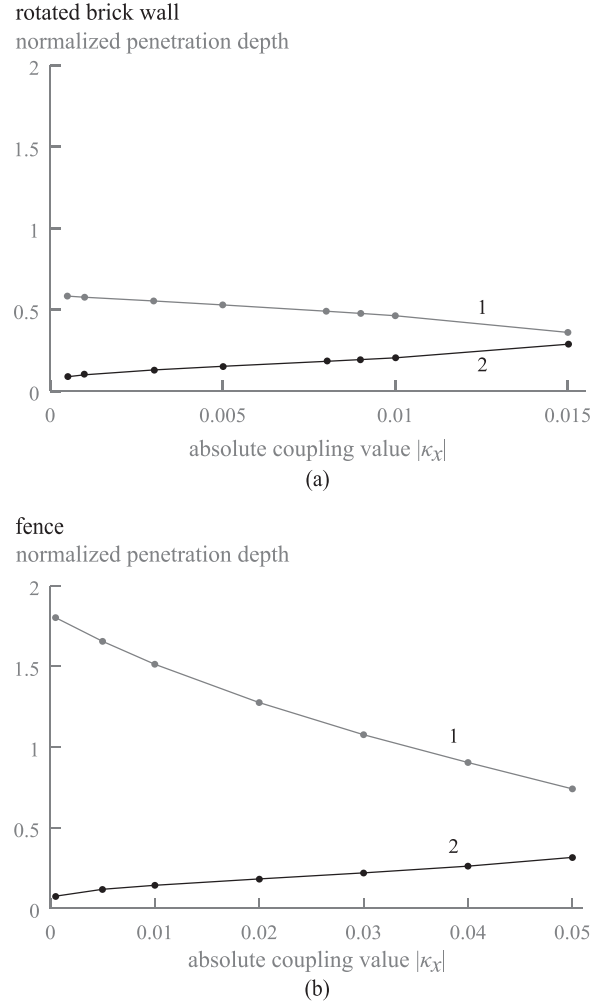


FIG. 8. For both modes, the penetration depth depends on the strength of the transverse coupling both for the rotated “brick-wall” (a) and the “fence” (b) metamaterials. As the coupling weakens, mode 2 penetrates less in the metamaterial, until they disappear. Mode 1, on the other hand, penetrates less in the metamaterial when the coupling is stronger. The normalized frequency is  $\omega/\omega_0 = 1.04$ .

Equation (11) plays the role of the boundary condition in the effective-medium model<sup>24</sup> and reduces to  $\mu_z k_{x1} = k_{x2}$  for small values of  $k_{x1}$  and  $k_{x2}$ .

For the “brick-wall” with the same parameters as in Sec. III, the complete circuit model gives a dispersion diagram of Fig. 10(a). It agrees well with the dispersion obtained from the effective-medium model [see Fig. 3(b)], especially at low wavenumbers where the periodic nature of the transmission line does not show, as the unit cell of the metamaterial is small  $k_z d \ll 1$ .

For the rotated “brick-wall,” the circuit model produces the dispersion diagram shown in Fig. 10(b). It has the same shape that the dispersion given by the effective-medium model [see Fig. 4(b)], although there are some quantitative differences. In particular, both dispersions behave in the same way as the transverse coupling increases: the region where the surface waves can propagate shrinks both in frequency and wavenumber [see Fig. 7(a)] and disappears when reaching a threshold value of the coupling coefficient.

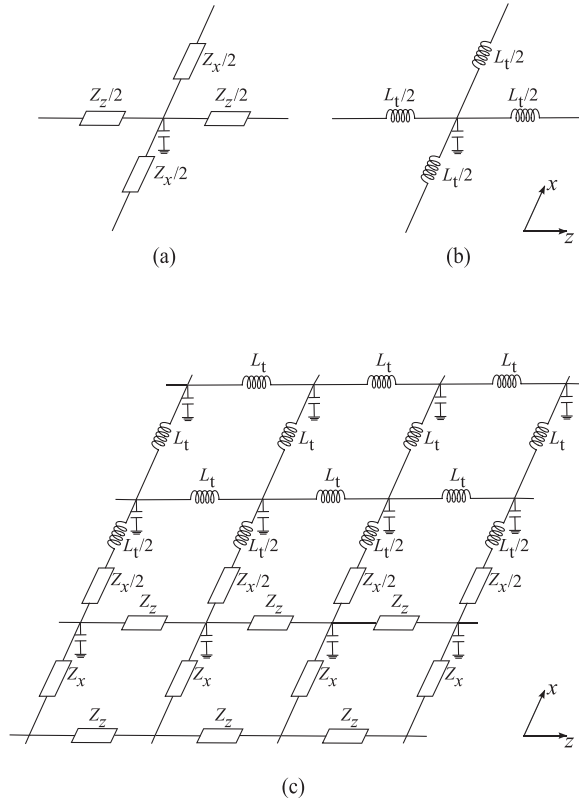


FIG. 9. In the equivalent-circuit model for surface polaritons, symmetric unit cells represent the metamaterial (a) and air (b), leading to the boundary (c).

Importantly, the dispersion diagram derived from the circuit model has the same boomerang form as in Fig. 4(b), indicating the presence of amplification in the circuit. It can only come from the load impedances  $Z_{Tx}$  and  $Z_{Tz}$ . Their values are purely imaginary (and, hence, lossless) as follows from Eq. (10), but their frequency derivatives  $dZ_{Tx}/d\omega$  and  $dZ_{Tz}/d\omega$  may become negative. It is shown in Fig. 11 for the two modes and for the parameters corresponding to  $\kappa_x = 0.009$  in Fig. 10(b). For mode 1, at least one of the derivative is negative close to the maximum and minimum values of the wavenumber. For mode 2, the derivative  $\partial Z_x/\partial\omega$  is negative for a wide range of the wavenumbers, which agrees with the results of the effective-medium model, cf. Fig. 4(b).

Circuits made of passive lossless components (Foster circuits<sup>34</sup>) can only have impedances for which  $d(\text{Im}Z)/d\omega > 0$ . Therefore, non-Foster circuits with active components are needed to realize the load impedances of Fig. 11 and allow surface waves to propagate. Active components allow one to realize negative inductances and capacitances and achieve the required  $d(\text{Im}Z_{Tx,z})/d\omega < 0$ . The presence of active components permits the existence of infinite group velocity, as seen at the left and right edges of the dispersion diagrams in Fig. 10(b). For another manifestation of super-luminal group velocities in *LC* transmission lines with negative capacitances, see Refs. 35 and 36. Metamaterials with non-Foster circuits, both with<sup>37,38</sup> and without<sup>35,39–41</sup> a resistor, have attracted attention.

This behavior of the load impedances mirrors the behavior of the permeabilities in the effective-medium

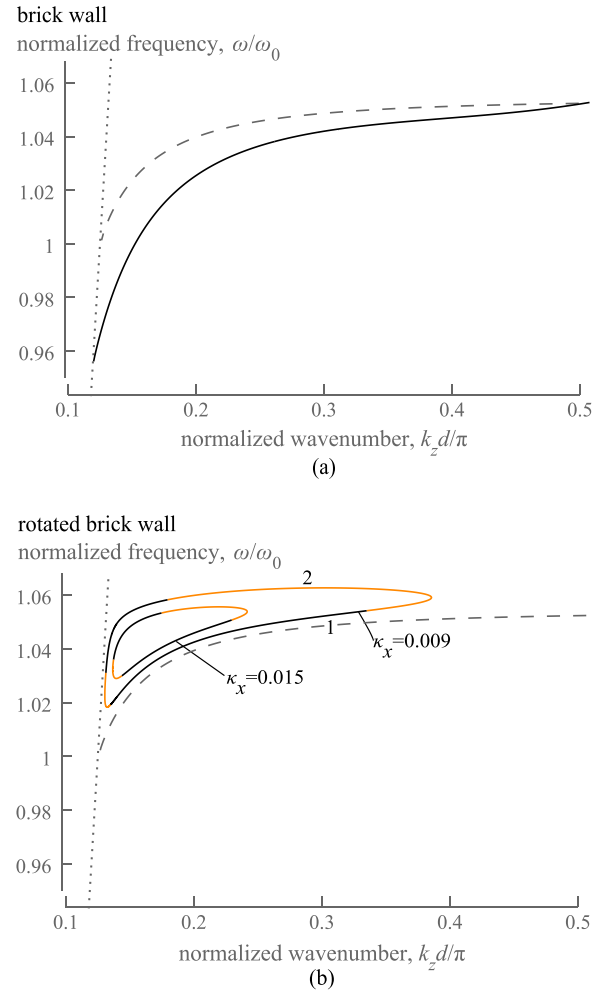


FIG. 10. The dispersion diagram of the “brick-wall” (a) and rotated “brick-wall” (b) metamaterials derived from the circuit model agree qualitatively well with the dispersion diagrams given by the effective-medium model, see Figs. 3 and 4. The sections where the frequency derivative of a load impedance becomes negative (see Fig. 11) are shown in orange.

model, see Fig. 6. The effective permeabilities were derived for bulk metamaterials, and as the equivalent model suggests, they may not always be appropriate for interface problems.

## V. CONCLUSIONS

This paper has discussed the propagation of surface polaritons along an interface between air and a magnetic metamaterial. The emphasis has been on the effects of the inter-element coupling. We have compared two models, one is based on an effective-medium approximation and bulk effective permeabilities of the metamaterial, and the other one is a full equivalent-circuit model. Both models were applied to a variety of metamaterials with different geometries of unit cells and relationships between the coupling coefficients.

According to both models, a moderate longitudinal coupling (along the interface) results in quantitative changes in the dispersion relation as compared to the metamaterial without inter-element coupling. However, the effect of the



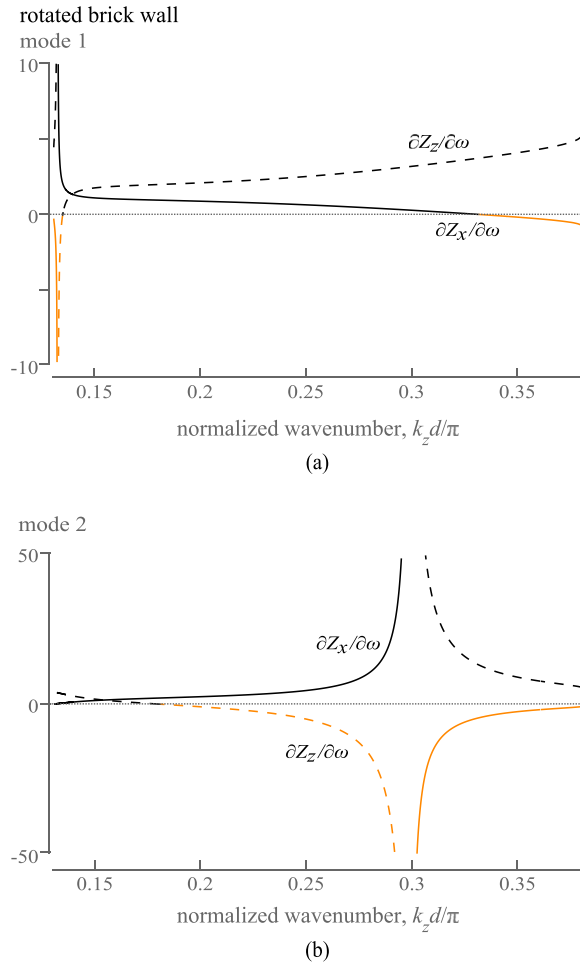


FIG. 11. The frequency derivative of the load impedances may become negative (shown in orange) for  $\kappa_x = 0.009$ , which indicates non-Foster active elements. This behavior mirrors the frequency derivatives of the effective permeabilities, see Fig. 6.

transverse coupling is much more dramatic. When the transverse coupling is weak, there are two branches of the dispersion diagram. For stronger transverse coupling, the dispersion characteristics dwindle, and no surface waves can propagate, an effect neglected by the models disregarding spatial dispersion.

However, similar to some previously reported metamaterial models,<sup>9</sup> the effective-medium approximation fails in some regions of frequencies and wavenumbers, leading to permeabilities suggesting an active media. The reasons for the failure became clear from the equivalent-circuit model. For a metamaterial with a transverse inter-element coupling, this model shows that surface eigenwaves can exist only if the metamaterial elements at the boundary are loaded by additional impedances. These impedances may demonstrate non-Foster behavior, thus requiring active elements. In agreement with the effective-medium model, the circuit model shows that no surface polaritons can propagate for strong transverse coupling regardless of the loads in the boundary layer.

In conclusion, both the effective-medium and the equivalent-circuit model showed that the inter-element coupling has a profound effect on the propagation of surface

polaritons. The models also highlight some dangers of using bulk effective parameters to describe surface electromagnetic phenomena in metamaterials.

## ACKNOWLEDGMENTS

The authors thank R. R. A. Syms and M. G. Silveirinha for helpful discussions. K.H. and S.A.M. gratefully acknowledge financial support from the Leverhulme Trust, and E.S. that from the DFG. The authors also thank the reviewers for valuable comments.

- <sup>1</sup>J. B. Pendry, A. J. Holden, W. J. Stewart, and I. Youngs, *Phys. Rev. Lett.* **76**, 4773 (1996).
- <sup>2</sup>J. B. Pendry, A. J. Holden, D. J. Robbins, and W. J. Stewart, *IEEE Trans. Microwave Theory Tech.* **47**, 2075 (1999).
- <sup>3</sup>C. R. Simovski, *J. Opt.* **13**, 013001 (2011).
- <sup>4</sup>M. I. Stockman, *Phys. Rev. Lett.* **98**, 177404 (2007).
- <sup>5</sup>V. M. Agranovich and V. Ginzburg, *Crystal Optics with Spatial Dispersion, and Excitons* (Springer, Berlin, 1984).
- <sup>6</sup>P. A. Belov, R. Marqués, S. I. Maslovski, I. S. Nefedov, M. Silveirinha, C. R. Simovski, and S. A. Tretyakov, *Phys. Rev. B* **67**, 113103 (2003).
- <sup>7</sup>C. R. Simovski and P. A. Belov, *Phys. Rev. E* **70**, 046616 (2004).
- <sup>8</sup>M. G. Silveirinha, *Phys. Rev. E* **73**, 046612 (2006).
- <sup>9</sup>M. G. Silveirinha, *Phys. Rev. B* **75**, 115104 (2007).
- <sup>10</sup>M. G. Silveirinha, *Phys. Rev. B* **76**, 245117 (2007).
- <sup>11</sup>M. G. Silveirinha and P. A. Belov, *Phys. Rev. B* **77**, 233104 (2008).
- <sup>12</sup>M. G. Silveirinha, J. D. Baena, L. Jelinek, and R. Marques, *Metamaterials* **3**, 115 (2009).
- <sup>13</sup>M. G. Silveirinha, *New J. Phys.* **11**, 113016 (2009).
- <sup>14</sup>*Electromagnetic Surface Modes*, edited by A. D. Boardman (Wiley, Chichester, 1982).
- <sup>15</sup>O. Sydoruk, E. Shamonina, V. Kalinin, and L. Solymar, *Phys. Plasmas* **17**, 102103 (2010).
- <sup>16</sup>E. Tatartschuk, N. Gneiding, F. Hesmer, A. Radkovskaya, and E. Shamonina, *J. Appl. Phys.* **111**, 094904 (2012).
- <sup>17</sup>E. Shamonina, V. A. Kalinin, K. H. Ringhofer, and L. Solymar, *J. Appl. Phys.* **92**, 6252 (2002).
- <sup>18</sup>L. Solymar and E. Shamonina, *Waves in Metamaterials* (Oxford University Press, 2009).
- <sup>19</sup>E. Tatartschuk, A. Radkovskaya, E. Shamonina, and L. Solymar, *Phys. Rev. B* **81**, 115110 (2010).
- <sup>20</sup>A. Radkovskaya, E. Tatartschuk, O. Sydoruk, E. Shamonina, C. J. Stevens, D. J. Edwards, and L. Solymar, *Phys. Rev. B* **82**, 045430 (2010).
- <sup>21</sup>G. I. Atabekov, *Linear Network Theory* (Pergamon Press, Oxford, 1965).
- <sup>22</sup>B. C. Knapp, E. A. Knapp, G. J. Lucas, and J. M. Potter, *IEEE Trans. Nucl. Sci.* **12**, 159 (1965).
- <sup>23</sup>J. S. Hong and M. J. Lancaster, *Microstrip Filters for RF/Microwave Applications* (Wiley-Interscience, New York, 2000).
- <sup>24</sup>E. Shamonina, *Phys. Rev. B* **85**, 155146 (2012).
- <sup>25</sup>R. R. A. Syms, E. Shamonina, V. Kalinin, and L. Solymar, *J. Appl. Phys.* **97**, 064909 (2005).
- <sup>26</sup>J. N. Gollub, D. R. Smith, D. C. Vier, T. Perram, and J. J. Mock, *Phys. Rev. B* **71**, 195402 (2005).
- <sup>27</sup>M. A. Shapiro, G. Shvets, J. R. Sirigiri, and R. J. Temkin, *Opt. Lett.* **31**, 2051 (2006).
- <sup>28</sup>N. Ilin, A. Smirnov, and I. Kondratiev, *Metamaterials* **3**, 82 (2009).
- <sup>29</sup>O. Sydoruk, A. Radkovskaya, O. Zhuromskyy, E. Shamonina, M. Shamonin, C. J. Stevens, D. J. Edwards, G. Faulkner, and L. Solymar, *Phys. Rev. B* **73**, 224406 (2006).
- <sup>30</sup>M. Gorkunov, M. Lapine, E. Shamonina, and K. H. Ringhofer, *Eur. Phys. J. B* **28**, 263 (2002).
- <sup>31</sup>O. Zhuromskyy, E. Shamonina, and L. Solymar, *Opt. Express* **13**, 9299 (2005).
- <sup>32</sup>G. V. Eleftheriades and K. G. Balmain, *Negative-Refractive Metamaterials: Fundamental Principles and Applications* (John Wiley and Sons, Hoboken, NJ, 2005).
- <sup>33</sup>C. Caloz and T. Itoh, *Electromagnetic Metamaterials: Transmission Line Theory and Microwave Applications* (John Wiley and Sons, Hoboken, NJ, 2005).

<sup>34</sup>R. M. Foster, [Bell Syst. Tech. J.](#) **3**, 259 (1924).

<sup>35</sup>S. Hrabar, I. Krois, I. Bonic, and A. Kirichenko, [Appl. Phys. Lett.](#) **99**, 254103 (2011).

<sup>36</sup>J. Long, M. M. Jacob, and D. F. Sievenpiper, [IEEE Trans. Microwave Theory Tech.](#) **62**, 789 (2014).

<sup>37</sup>K. Z. Rajab, Y. Hao, D. Bao, C. G. Parini, J. Vazquez, and M. Philippakis, [J. Appl. Phys.](#) **108**, 054904 (2010).

<sup>38</sup>S. Hrabar, I. Krois, I. Bonic, and A. Kirichenko, [Appl. Phys. Lett.](#) **102**, 054108 (2013).

<sup>39</sup>S. A. Tretyakov, [Microwave Opt. Technol. Lett.](#) **31**, 163 (2001).

<sup>40</sup>M. Barbuto, A. Monti, F. Bilotti, and A. Toscano, [IEEE Trans. Antennas Propag.](#) **61**, 1219 (2013).

<sup>41</sup>P.-Y. Chen, C. Argyropoulos, and A. Alu, [Phys. Rev. Lett.](#) **111**, 233001 (2013).